mm-Wave Op-Amps employing simple-Miller compensation, with OIP3/P$_{DC}$ ratios of 211 (10 dB NF) and 144 (6.0 dB NF) at 2 GHz

Zach Griffith*, Miguel Urteaga*, and Mark J.W. Rodwell†
*Teledyne Scientific and Imaging Company
1049 Camino Dos Rios, Thousand Oaks, CA 91360, USA
E-mail: zgriffith@teledyne.com

†Dept. of Electrical and Computer Engineering, University of California, Santa Barbara, CA 93106-9560, USA

***Abstract*— We here report two mm-wave amplifiers employing strong global negative feedback to provide very low intermodulation distortion, using a 500 nm InP DHBT technology. The amplifiers, similar to operational amplifiers, use simple-Miller compensation and have 25 to 35 GHz feedback loop bandwidths. The large loop transmission at 2 GHz provides a large reduction of closed-loop distortion at this frequency.**

The first amplifier, designed for lowest IM3 distortion at this technology node, showed 35 GHz bandwidth, 13.8 dB (S$_{21}$) gain, with 1005 mW dissipation – where 53.2 dBm OIP3 and 10 dB NF are observed at f_1, f_2 = 1.950, 1.975 GHz. It is unconditionally stable from DC to 15 GHz. The second amplifier improves upon noise figure through less-strong feedback and minimal input padding resistance, showing 25.8 GHz bandwidth, 19.8 dB (S$_{21}$) gain, with 956 mW dissipation – where 51.4 dBm OIP3 and 6 dB NF are observed at f_1, f_2 = 1.950, 1.975 GHz. It is unconditionally stable from DC to 8 GHz. These results represent a $\sim$ 1.4× bandwidth increase for an op-amp employing simple-Miller compensation, *as well as* $\sim$ 2.0 and 1.4× betterment in OIP3/P$_{DC}$ ratio at f_s = 2-3 GHz, compared to state-of-the-art.

We address considerations important to the application of negative feedback to mm-, microwave amplifiers, including the effects of interface impedances on stability, the effect of feedback upon return losses and noise figure, and the effect of frequency compensation and of feedback topology on closed-loop distortion.

***Index Terms*— operational-amplifier, Miller compensation, intermodulation distortion**

I. INTRODUCTION

Amplifiers with very low intermodulation distortion are required in radar receivers and in multi-carrier communications systems such as cell phone base stations. In simple reactively-tuned RF amplifiers the output-referred third-order intermodulation distortion intercept (OIP3) is proportional to the DC current dissipation. In this situation very low IM3 can be obtained only at the cost of high DC power consumption.

Here we report mm-wave (2 GHz) amplifiers having high (greater than 51 dBm) third-order intermodulation intercepts despite consuming a relatively low $\sim$ 1000 mW power dissipation P_{DC}. This very high ratio of output-referred third-order-intercept power to DC power consumption $P_{OIP3}/P_{DC} > 200$ is obtained through the use of strong global negative feedback using circuit techniques similar to classic operational amplifiers [1]. We explicitly distinguish this work from that of other mm-, microwave feedback amplifiers using a feedback resistor $R_f = Z_o(1 - A_v)$ [2] to provide a matched Z_o input impedance; such amplifiers have less than unity feedback magnitude. In marked contrast, low amplifier distortion is here obtained using strong global negative feedback; a mm-wave *operational amplifier*.

Obtaining high OIP3 requires novel designs and detailed attention to residual sources of distortion. Because 20-40 GHz loop bandwidths are required, stability is critically sensitive to layout and interconnect parasitics. Frequency compensation limits the degree of reduction of output-stage distortion and increases the distortion associated with stages nearer the input. Difficulties arise from inadvertent non-linear loading of the feedback network by transistor junction capacitances. Challenges include the control of input and output impedances, and the sensitivity of the loop bandwidth – i.e. phase margin to generator and load impedances. Manufacturable InP heterojunction bipolar transistor (HBT) IC technologies offer cutoff frequencies $\geq$ 350 GHz [3]. With appropriate design, stable feedback loops of $\sim$ 40 GHz bandwidth can be realized, providing strong feedback at low GHz operation for strong distortion suppression.

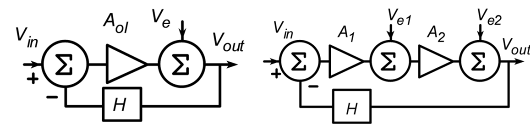

(a) (b)

Fig. 1. Error (distortion) analysis of feedback amplifiers: (a) single-stage and (b) multi-stage feedback amplifier with global feedback.

Prior to the results reported here, the authors have reported in [4] similar op-amps utilizing simple-Miller compensation with 24.8 GHz bandwidth, 13.8 dB (S$_{21}$) gain, with 1013 mW dissipation – where 50.2 dBm OIP3 and 11 dB NF were observed at f_1, f_2 = 1.950, 1.975 GHz. Extending upon this work, we here report two simple-Miller compensated op-amps with reduced IM3 distortion. The first amplifier has been designed for highest OIP3 at this technology node and showed 35 GHz bandwidth, 13.8 dB (S$_{21}$) gain, with 1005 mW dissipation – where 53.2 dBm OIP3 and 10 dB NF are observed at f_1, f_2 = 1.950, 1.975 GHz. This bandwidth reflects 1.4× betterment in state-of-the-art for a simple-Miller compensated op-amp. The second amplifier, similar the first, has been modified for reduced noise figure using less strong feedback and minimal input padding resistance. It shows 25.8 GHz bandwidth, 19.8 dB (S$_{21}$) gain, with 956 mW dissipation – where 51.4 dBm OIP3 and 6 dB NF are observed at f_1, f_2 = 1.950, 1.975 GHz. When compared to the previous work from our laboratory, the OIP3/P$_{DC}$ ratios of 211 and 144 here reflect 2.0× and 1.4× betterment in state-of-the-art.

II. THEORY

An amplifier (fig. 1a) having open-loop distortion V_e produces a closed-loop output of $V_{out} = A_{CL}V_{in} + (A_{CL}/A_{OL})V_e$, where $A_{CL} \cong 1/H$ is the closed-loop gain. Distortion is reduced by the ratio (A_{CL}/A_{OL}) of closed-loop to open-loop gain. In a two-stage design (fig. 1b) each stage first produces open-loop intermodulation distortion (V_{e1}, V_{e2}) determined by the magnitude of the stage output signals (V_{out1}, V_{out2}) and third-order intercepts $(V_{OIP3,1}, V_{OIP3,2})$ through the relationships $V_{e2} = V_{out2}^3/V_{OIP3,2}^2$ and $V_{e1} = V_{out1}^3/V_{OIP3,1}^2 = (V_{out}/A_{V,2})^3/V_{OIP3,1}^2$. The closed-loop output is then $V_{out} = A_{CL}V_{in} + (A_{CL}/A_1)V_{e1} +$

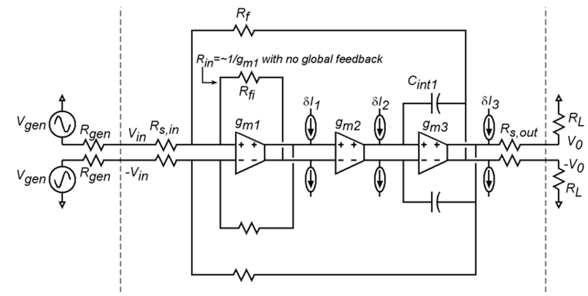

Fig. 2. Current-mode operational amplifier in simple-Miller form using HBT differential g_m blocks. Amplifier distortion currents are illustrated.

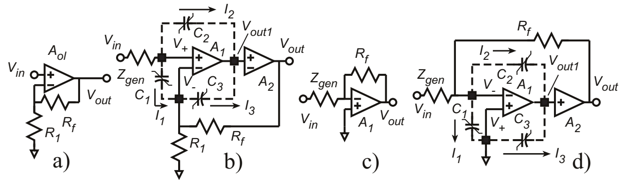

Fig. 3. Distortion from some non-linear impedances is not reduced by feedback. An elementary voltage-sum amplifier (a), when loaded by the non-linear input-stage capacitances (b) suffers from non-linear loading of the feedback network. An elementary current-sum amplifier (c), if constructed in multi-stage form (d) avoids these effects.

$(A_{CL}/A_1A_2)V_{e2}$. The amplifier must be frequency compensated for stability, $A_1A_2H = f_{unity}/jf$, by making either A_1 or A_2 vary at $1/jf$. In the first case if $A_1 \propto 1/jf$, the closed-loop distortion terms $(A_{CL}/A_1)V_{e1}$ and $(A_{CL}/A_1A_2)V_{e2}$ increase at high frequencies. In the second case if $A_2 \propto 1/jf$ for constant V_{out2}, V_{out1} varies as jf and V_{e1} consequently varies as $(jf)^3$ [5]. Distortion in either case increases at high frequencies.

The amplifiers in this work are in current-mode form and use simple-Miller compensation (fig. 2). The blocks g_{m1}, g_{m2} are degenerated HBT differential pairs; the output stage (g_{m3}) is a differential pair having emitter-follower input buffers. When brought together, the simple-Miller amplifier consists of the g_{m2}, g_{m3} Miller integrators, and a transimpedance input stage (g_{m1}).

We now extend the earlier distortion analysis. Assume that $R_{s,out} << R_L$. With a two-tone $(f_1 = f_s + \varepsilon, f_2 = f_s - \varepsilon)$ output signal, where each tone is of root-mean-square (RMS) amplitude V_{out}, the RMS currents of (g_{m1}, g_{m2}, g_{m3}) at f_1 and at f_2 are $I_{out3} \cong (1/R_L + j2\pi f_s C_{int1})V_{out}$, $I_{out2} \cong j2\pi f_s C_{int1} V_{out}$, and $I_{out1} \cong j2\pi f_s (C_{int1}/g_{m2}R_{fi})V_{out}$. Because of the $I_c = I_s \exp(qV_{be}/\eta kT)$ HBT characteristics, each stage produces distortion currents $(\delta I_1, \delta I_2, \delta I_3)$ at $(2f_1 - f_2, 2f_2 - f_1)$ of RMS amplitudes $\delta I_1 = I_{out1}^3/I_{OIP3,1}^2$, $\delta I_2 = I_{out2}^3/I_{OIP3,2}^2$, and $\delta I_3 = I_{out3}^3/I_{OIP3,3}^2$ – where each stage's output-referred IP3 is simply its DC bias current. The amplifier closed-loop gain is $A_{CL} = V_{out}/V_{gen} = R_f/(R_{gen}+R_{s,in})$, while $S_{21} \cong 2R_f/(Z_o + R_{s,in})$. The closed-loop output voltage contains frequency components at $(2f_1 - f_2, 2f_2 - f_1)$, each of RMS amplitude δV_{out}, where

$$\delta V_{out} = \left(\frac{\delta I_3}{g_{m3}}\right)\left(\frac{jf}{f_{unity1-2-3}}\right) + \left(\frac{\delta I_2}{g_{m2}}\right)\left(\frac{R_f}{R_{fi}}\right) + \left(\frac{\delta I_1}{g_{m1}}\right)\left(\frac{R_f}{R_{s,in}+R_{gen}} + \frac{R_f}{R_{fi}}\right) \quad (1)$$

where $f_{unity1-2-3} \cong (g_{m2}R_{fi}/C_{int1}R_f)$ is the unity-gain frequency of the feedback loop transmission, where $T \sim f_{unity1-2-3}/jf$. In a 350 GHz f_τ, f_{max} HBT technology, $f_{unity1-2-3} \sim$ 25-40 GHz are feasible. At $f_s \sim$ 2 GHz, considerable reduction in the output stage distortion is therefore feasible.

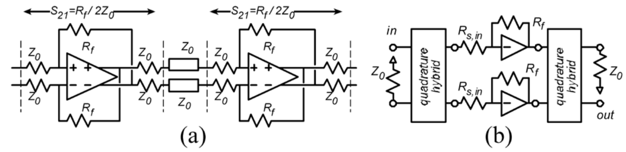

Fig. 4. Managing input and output impedances by (a) transmission-line series termination and (b) through the balanced amplifier configuration.

Note: compensation strongly impacts distortion, as the 2^{nd}-stage output current is $I_{out2} \cong j2\pi f_s C_{int1} V_{out}$ and becomes large at high frequencies. Additionally, hand analysis for the simple-Miller-compensated amplifier correlates very well with computer simulation and experimental data.

Space prevents us from here addressing the general effects of non-linearities associated with the HBT junction capacitances C_{cb} and C_{je}. The effect of non-linear capacitive loading of the feedback network is however of paramount importance. In a simple series-shunt feedback amp (fig. 3a), low distortion is not obtained even with strong feedback. Considering separately (fig. 3b) the effect of the input (A_1) and subsequent (A_2) stages, in the limit of large loop gain $T = A_1A_2R_1/(R_f + R_1) \rightarrow \infty$; the differential input signal $(V^+ - V^-)$ is driven to zero, driving to zero the current I_1 associated with the non-linear input capacitance C_1. The voltages $(V^+ - V_{out1})$ and $(V^- - V_{out1})$ are driven *not to zero* but to $V_{in}(1 - A_{CL}/A_2)$ as $T \rightarrow \infty$; hence the currents (I_1, I_2) flowing through the input stage's non-linear base-collector capacitances (C_2, C_3) also remain nonzero. These currents (I_1, I_2) produce voltage drops across the feedback network impedances (Z_{gen}, R_1, R_f), producing closed-loop distortion even in the limit $T \rightarrow \infty$. The shunt-shunt feedback amplifier (fig. 3c,d) avoids this limitation – in the limit $A_2 \rightarrow \infty$, the voltages $(V^+ - V^-)$, $(V^+ - V_{out1})$, and $(V^- - V_{out1})$ are all driven to zero, forcing $(I_1, I_2, I_3) \rightarrow 0$. Our designs therefore use the shunt-shunt configuration.

The generator and load impedances will change the loop transmission T; unfavorable values may cause oscillation. We must clearly distinguish between stability in a 50 Ω system and stability with arbitrary generator and load (unconditional stability) impedance. Even before applying global feedback, the *open-loop* output impedance is low because of the local feedback through C_1; hence even ~5-10 Ω series padding $R_{s,out}$ provides a large range of *load* impedances for which the loop is stable. The transimpedance input stage (g_{m1}) provides an *open-loop* input impedance $R_{in,open-loop} \cong 1/g_{m1}$; provided that $||Z_{gen} + R_{s,in}|| < 1/g_{m1}$, T is then only weakly dependent upon Z_{gen}. This provides a wide range of *generator* impedances for which the loop is stable. Additionally, because the loop bandwidth is ~20-40 GHz while $f_s \sim$ 2 GHz, unconditional stability can be obtained by isolating at high frequencies the feedback amplifier from the external load using frequency-selective networks – as is standard in audio power amplifiers.

Finally, note that the shunt-shunt feedback forces $Z_{in} \rightarrow R_{s,in}$ and $Z_{out} \rightarrow 0$ Ω. If impaired noise figure and output power can be accepted, matched line interfaces can be provided by series padding (fig. 4a). For highest OIP3 and lowest noise figure, one must set $R_{s,in} << Z_o$ and $R_{s,out} << Z_o$, which leads to poor S_{11} and S_{22}. In this case, a balanced amplifier configuration (fig. 4b) will provide low return losses over many octave of bandwidth even with minimal or zero series input and output padding.

III. Design

A simple resistive feedback network is used for these circuits. To ensure the network remains dominantly real across the 3dB bandwidth of the op-amp, the length of the feedback path (Z_o = 50 Ω) is only 65 μm in order to avoid series inductance or shunt capacitance loading on the interconnect. Such a short length is possible with the symmetric, folded floorplan used for circuit layout,

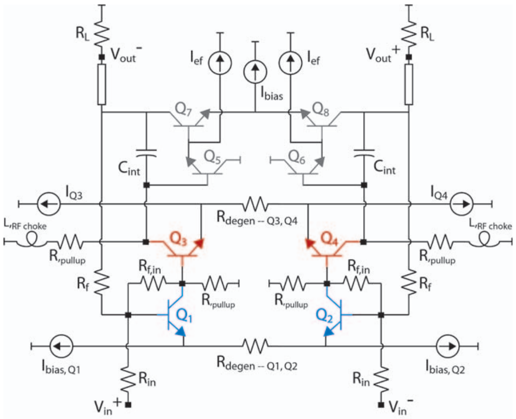

Fig. 5. Circuit floorplan of the simple-Miller-compensated op-amp.

TABLE I

BIAS DETAILS FOR THE SIMPLE-MILLER COMPENSATED OP-AMPS.

V_{ee}=-4.5 V	stage 1	stage 2	stage 3,EF	stage 3,diff
$I_{Q\ x,y}$ (mA)	10	30	14	56
P_{DC} (mW)	90	270	126	504

shown in figure 5. Compared to the previous results reported in [4], amplifier designs were pursued that continued to suppress IM3 distortion (even in the presence of $\sim$ 10 dB NF), as well as designs with similar 50 dBm OIP3 as [4] but with only 6 dB noise figure. By adjusting the gain $g_{m,i}$ of the respective stages more towards the amplifier input (while keeping the open-loop gain greater than or equal to the designs in [4]), distortion has been reduced. Circuit simulation revealed the dominant sources of noise were the input padding resistor R_{in} and $R_{degen,Q1,Q2}$ – appropriate reductions were made to satisfy the 6 dB noise figure design goal. For the amplifier with strongest feedback and lowest IM3, R_f = 300 Ω, R_{in} = 50 Ω, and $R_{f,in}$ = 250 Ω. For the amplifier with less strong feedback and reduced input padding, R_f = 350 Ω, R_{in} = 5 Ω, and $R_{f,in}$ = 350 Ω with 5.5 dB simulated NF.

The bias currents for the simple-Miller compensated op-amp are set by using pulldown resistors and the bias voltage at the base for a given amplifier stage is set by the potential drop $I_{Q,i}R_{pullup,i}$ of the preceeding stage. Because the bias current of stage-2 is large, $R_{pullup,2}$ must be small to correctly set the stage-3 voltage. To avoid the large distortion current associated with having only small $R_{pullup,2}$ load the collector of stage-2 (in parallel with stage-3 input), *and* to increase stage-2 gain for higher A_{ol}, a 10 nH inductor is placed in-series to act as an RF choke where $Z = R_{pullup,2}+j\omega L$, as *pnp* HBTs are not available. To improve the output return-loss and amplifier stability, 7.5 Ω of series output padding is used.

Details of the InP HBT process from Teledyne Scientific have been reported [3], where inverted, thin-film dielectric (Benzocyclobutene, 3 μm thick) microstrip wiring is employed and the topmost metal layer is used as the ground plane. Both amplifiers are biased by a single voltage source -4.5 V_{ee}, and voltage offsets V_{in} $\cong$ -2.15V and V_{out} $\cong$ -460mV are required. Table I summarizes the biasing (I_Q and P_{DC}) of the various stages in the amplifiers.

IV. MEASUREMENT SETUP

4-port RF measurements of the circuits were performed using a 10MHz-50GHz (Agilent E8364B, N4421B) network analyzer after SOLT calibration.

For two-tone power and IM3 measurements, the test-bench here employs two synthesizers operating at 1.950 and 1.975 GHz. Their respective outputs pass through 6dB of attenuation, a low-pass filter, and two 20dB isolators before being brought together by a power combiner. A differential two-tone signal is created by way of a 180° hybrid-ring and applied on-wafer. The differential output is combined and measured. Output loss associated with the cabling and hybrid-ring between the probes and spectrum analyzer was measured by 3-port S-parameters and is 4.7 dB. Measurement of a differential thru-line shows 56 dBm OIP3 of residual system distortion.

Noise figure measurements are performed using an Agilent 3466 noise source and 8971C noise test set in the presence of the aforementioned 180° hybrid-rings for differential signal generation. Once the noise source and test-set have been calibrated, circuit measurements are performed. The noise figure of the op-amp is extracted through the use of Friis' equation [6] so we may deembed the cascaded stages of the input and output (effective 2-port) hybrid rings.

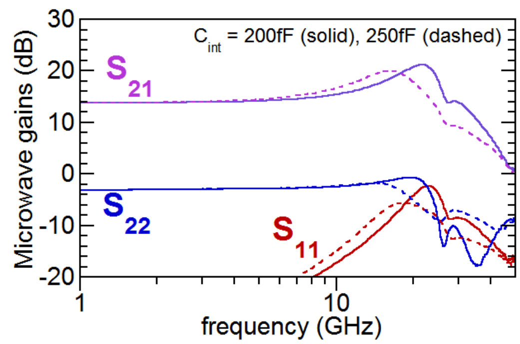

(a) S-parameters for op-amps with strongest feedback.

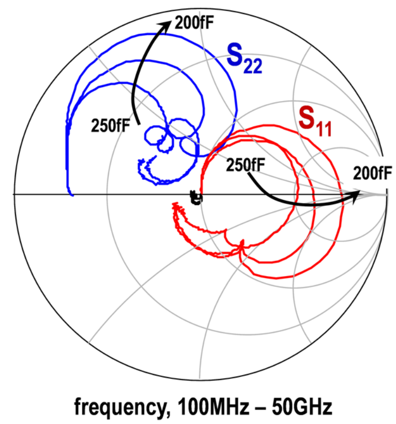

(b) S-parameters, Smith chart format.

Fig. 6. Measured differential RF characteristics for the single-Miller compensated op-amp with strongest feedback. The loop-bandwidth is varied through compensation only, where C_{int} = 200, 225, and 250 fF.

V. OP-AMP CIRCUIT RESULTS

Figure 6 shows the microwave gains of the op-amps designed for highest OIP3 at this 500nm InP DHBT technology node. The nominal S_{21} gain is 13.8dB and P_{DC} = 1005 mW. As the loop bandwidth is varied through compensation C_{int} = 250, 225, 200fF, the respective amplifier 3dB bandwidths are 26.0 GHz (6.1 dB peaking), 35.0 GHz (5.0 dB peaking), and 35.0 GHz (7.5 dB peaking). From the Rollett stability factor K, these amplifiers are

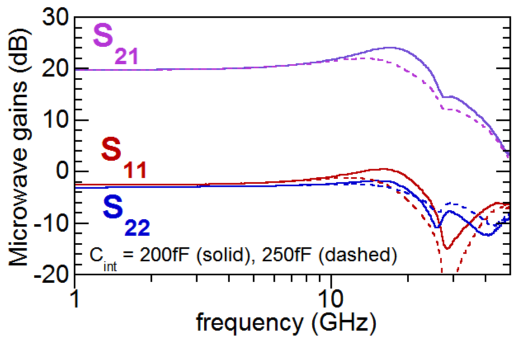

(a) S-parameters for op-amps with less strong feedback and minimal input padding resistance.

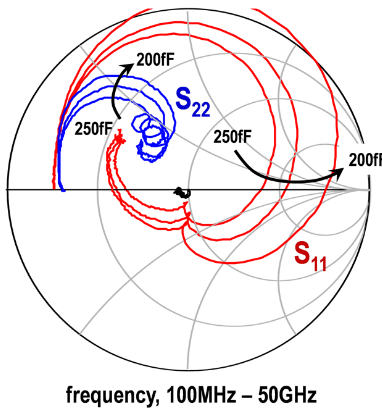

(b) S-parameters, Smith chart format.

Fig. 7. Measured differential RF characteristics for the single-Miller compensated op-amp with less strong feedback and minimal input padding resistance for reduced noise figure. The loop-bandwidth is varied through compensation only, where C_{int} = 200, 225, and 250 fF.

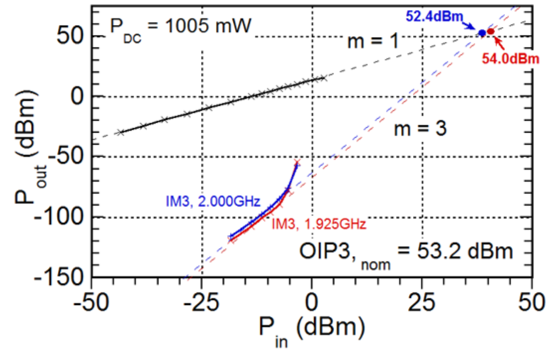

(a) Power measurements of the op-amp with strongest feedback (lowest IM3 distortion), whose RF data is shown in fig. 6. C_{int} = 200 fF.

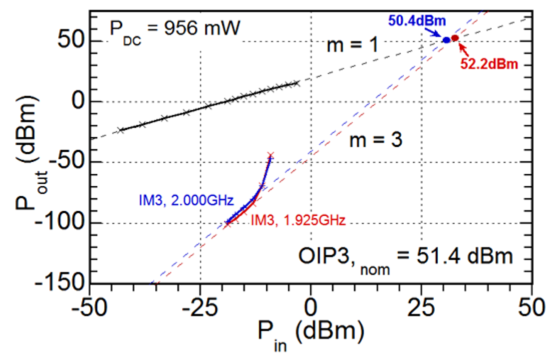

(b) Power measurements of the op-amp with less-strong feedback and reduced input padding resistance (lowest noise), whose RF data is shown in fig. 7. C_{int} = 200 fF.

Fig. 8. Two-tone power (f_1, f_2 = 1.950, 1.975 GHz) and IM3 measurements (f_{IM3} = 1.925, 2.000 GHz) of the simple-Miller compensated op-amps.

unconditionally stability from DC-15 GHz and conditionally stable in a 50 Ω environment across the 50 GHz measurement span.

Figure 7 shows the microwave gains of the op-amps designed for 6 dB NF and OIP3 $\geq$ 50 dBm. The nominal S_{21} gain is 19.8dB and P_{DC} = 956 mW. As the loop bandwidth is varied through compensation C_{int} = 250, 225, 200fF, the respective amplifier 3dB bandwidths are 24.1 GHz (2.3 dB peaking), 25.1 GHz (3.0 dB peaking), and 26.0 GHz (4.4 dB peaking). From the Rollett stability factor K, these amplifiers are unconditionally stability from DC-8 GHz and conditionally stable in a 50 Ω environment across the 50 GHz measurement span – with exception of the C_{int} = 200 fF design where $S_{11} > 0$ dB between 13-18 GHz.

Differential two-tone power measurements ($f_{1,2}$ = 1.950, 1.975 GHz) for both versions of the op-amp (C_{int} = 200 fF) are shown in figure 8. The expected P_{in} versus P_{out} trends for the fundamentals and IM3 products (f_{IM3} = 1.925, 2.000 GHz) are clearly observed, and the intercept superimposed on the graph agrees very well with the OIP3 calculation from discrete values of P_{in}.

For the op-amp with lowest IM3 distortion, measurements show the OIP3 is 53.2 dBm (fig. 8a) – where its OIP3 to P_{DC} ratio is 211, and its NF = 10 dB. For the op-amp utilizing reduced padding resistance and feedback, the OIP3 is 51.4 dBm (fig. 8b) – where its OIP3 to P_{DC} ratio is 144, and its NF = 6.0 dB. The results here represent a 2.0 and 1.4× betterment in state-of-the-art [4] at similar operating frequencies. As the output power of each tone approaches 8.3 dBm for the highest OIP3 design (6.6 dBm for the lowest NF design), higher order IM_X distortion dominates as the output stage HBTs are beginning to operate into quasi-saturation (Kirk-effect, non-linear C_{cb}). The P_{1dB} compression under two-tone drive is 15.0 dBm per tone for all amplifiers reported.

Acknowledgment

This work was supported by the DARPA FLARE program. Special thanks to Program Managers Dr. Sanjay Raman and Dr. Steve Pappert, and Dr. Richard Eden for their contributions and support.

References

[1] J.E. Solomon *et al.*, *IEEE Journal of Solid-State Circuits*, Vol. SC-9, No. 6. Also at http://www.national.com/an/AN/AN-A.pdf

[2] M.J.W. Rodwell *et al.*, *Journal of Solid-State Circuits*, Vol. 26, No. 10, pp. 1378-1382, October 1991.

[3] M. Urteaga *et al.*, *Proc. Device Research Conf.*, Notre Dame, IN, pp. 239-240, June 21-23, 2004.

[4] Z. Griffith *et al.*, *Proc. Indium Phosphide and Related Materials Conf.*, Versailles, France, May 25-29, 2008.

[5] E. Cherry, *IEEE Transactions on Acoustics, Speech, and Signal Process*, Vol. 29, Iss. 2, Apr. 1981, pp. 137-146.

[6] A. van der Ziel, *Noise: Sources, Characterization, Measurement.* Englewood Cliffs, NJ, Prentice-Hall, 1970.